Supporting Information for

Kinetic Modeling of Spillover and Temperature-Programmed Oxidation of Oxy-Carbon Surface Species on Pt/Al_2O_3

Casey P. O'Brien, Ivan C. Lee*

U.S. Army Research Laboratory, Sensors and Electron Devices Directorate, 2800 Powder Mill Road, Adelphi, MD 20783, USA

Table of Contents

S.1. Time-resolved DRIFTS spectra collected at all reaction conditions……..…...…….S3

S.2. Oxy-carbon surface species growth curves at all reaction conditions……...……S4

S.3. Carbon growth parity plot……...S6

S.4. Reverse spillover model for TPO of oxy-carbon species……S7

S.5. Evidence for Pt surface reaction-limited TPO kinetics……..S9

S.6. Temperature-programmed oxidation simulation details…….S12

S.7. Parity plots for TPO profiles…….S15

S.8. TPO of oxy-carbon species from deactivated Pt/Al_2O_3……S16

S.9. Parity plot for TPO of oxy-carbon species on the deactivated Pt/Al_2O_3 catalyst……...S17

References……...S18

S.1. Time-resolved DRIFTS spectra collected at all reaction conditions

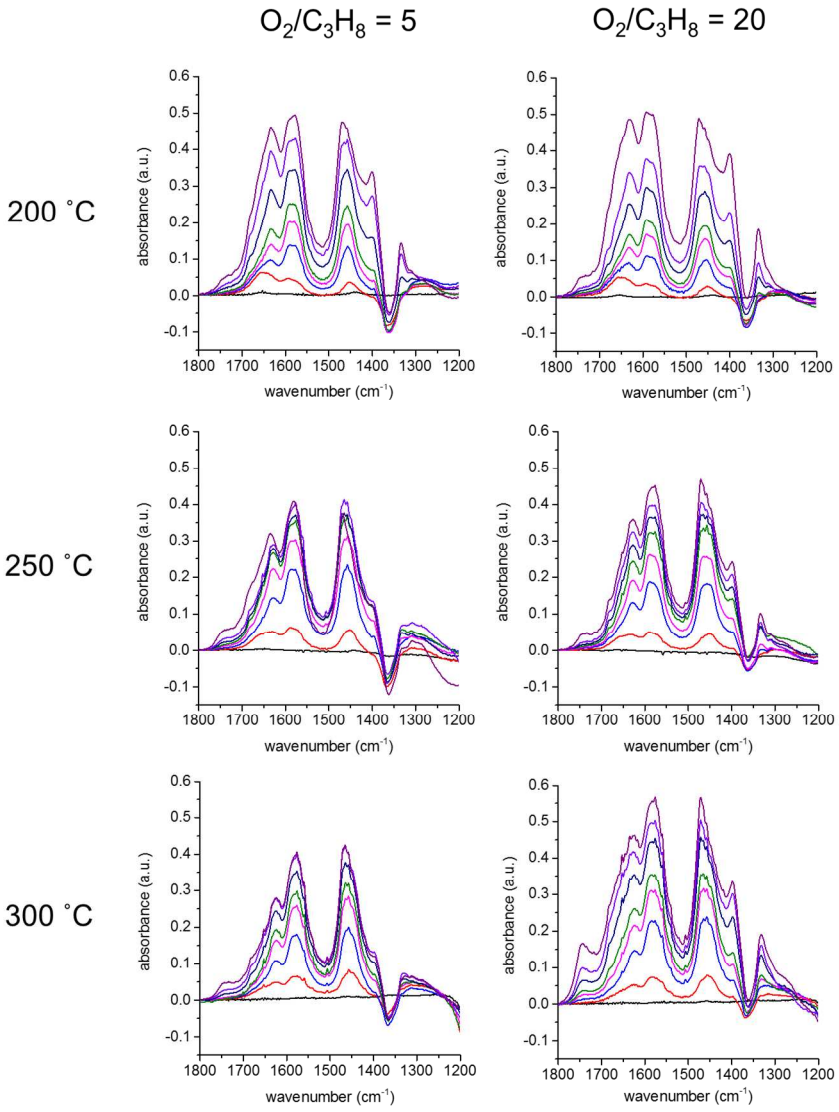

Figure S1. DRIFTS spectra collected during propane oxidation over Pt/Al_2O_3 at 200 ˚C (top row), 250 ˚C (middle row), and 300 ˚C (bottom row), and with O_2/C_3H_8 equal to 5 (left column) and O_2/C_3H_8 equal to 20 (right column). Line colors correspond to the following propane oxidation times: black (0 min), red (1 min), blue (10 min), magenta (20 min), olive (30 min), navy (60 min), violet (120 min), and purple (400 min). All spectra have been reported in the supporting information of a previous publication [1].

S.2. Oxy-carbon surface species growth curves at all reaction conditions

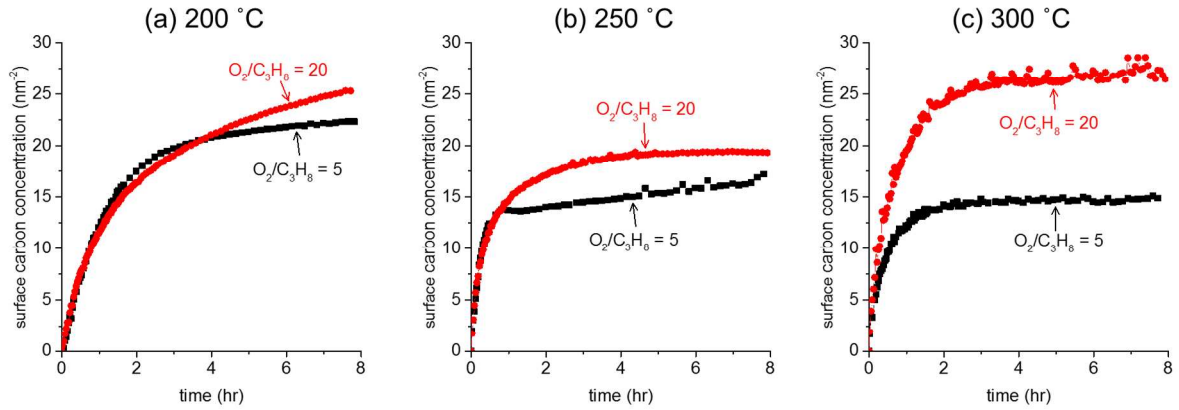

Figure S2. Surface carbon concentration versus time during propane oxidation over Pt/Al_2O_3 with O_2/C_3H_8 equal to 5 (black) and red (20), and at (a) 200 ˚C, (b) 250 ˚C, and 300 ˚C. The surface carbon concentration was obtained by integrating the time-resolved spectra in Figure S4 and converting to surface carbon concentration using Equation S9. The surface carbon growth curves have been reported in the supporting information of a previous publication [1].

The oxy-carbon surface species concentration is dependent on the O_2/C_3H_8 ratio at longer reaction times and at higher temperatures (see Figure S2), which is not explicitly accounted for in the spillover model, Equation (6). This observation can be rationalized by considering that the oxy-carbon surface species coverage is determined by the difference in the rates of oxy-carbon species growth (i.e. diffusion) on the Al_2O_3 support and oxy-carbon species oxidation to CO_2. The rate of oxy-carbon species diffusion on the Al_2O_3 support is independent of the O_2/C_3H_8 ratio, but the rate of oxy-carbon species oxidation at the platinum nanoparticles is dependent on the oxygen coverage on the platinum nanoparticles via the O_2/C_3H_8 ratio. At 200 ˚C, the rate of oxy-carbon species oxidation to CO_2 is negligible and, therefore, the rate of oxy-carbon species growth is dominated by the rate of oxy-carbon species diffusion on the Al_2O_3 support, which is independent of the O_2/C_3H_8 ratio. At higher temperatures, however, the rate of oxy-carbon species oxidation becomes more significant and therefore, the rate of oxy-carbon species growth depends more significantly on the O_2/C_3H_8 ratio. The influence of O_2/C_3H_8 ratio on the growth

of oxy-carbon species is more significant at longer reaction times because, at the beginning of the reaction, diffusion of oxy-carbon species on the Al_2O_3 support dominates the overall rate of oxy-carbon species growth. As the coverage of oxy-carbon species increases with increasing reaction time, the rate of oxy-carbon species diffusion decreases, and the influence of the rate of oxy-carbon species oxidation to CO_2 on the overall rate of oxy-carbon species growth becomes more significant.

S.3. Carbon growth parity plot

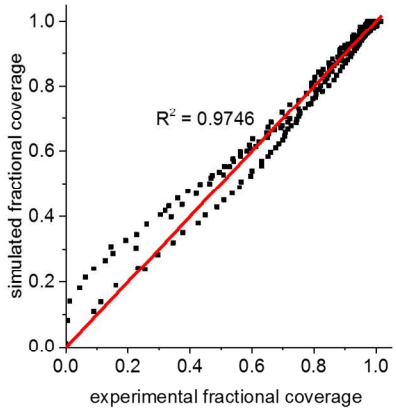

Figure S3. Parity plot comparing the simulated and experimental fraction of equilibrium coverage of oxy-carbon surface species during propane oxidation at 200 ˚C, 250 ˚C, and 300 ˚C.

S.4. Reverse spillover model for TPO of oxy-carbon species

The reverse spillover model for modeling temperature-programmed oxidation (TPO) of oxy-carbon surface species is

$$F(t) = 4\sum_{n=1}^{\infty} \frac{1}{\alpha_n^2} \exp\left[-\frac{D(t)}{R_S^2}\alpha_n^2 t\right] \qquad \text{(S1)}$$

where $F(t)$ is the fraction of equilibrium coverage of oxy-carbon surface species, the α_n's are the zeros of the Bessel function of the first kind of order zero, t is time, and R_S is the radius of the spillover zone at equilibrium coverage, which we assumes is ~$2.8 \cdot 10^{-6}$ cm based on TEM images. The diffusion coefficient ($D(t)$) is used with the pre-exponential factor and the activation barrier extracted from kinetic analysis of oxy-carbon species spillover:

$$D(t) = \left(7.9 \cdot 10^{-14}\,\frac{cm^2}{s}\right) \cdot \exp\left(\frac{-24\frac{kJ}{mol}}{R(T_0+\beta t)}\right) \qquad \text{(S2)}$$

During TPO the temperature increases from the intial temperature (T_0) at a constant rate (β) of 25 K/min. The instantaneous rate of CO_2 production (s^{-1}) at time t_m during TPO can then be calculated according to

$$r_{CO_2}(t_m) = C_{eq}[F(t_{m-1}) - F(t_m)] \qquad \text{(S3)}$$

Where C_{eq} represents the concentration of oxy-carbon surface species (per-Pt-site) at equilibrium, which is also equal to the total amount of carbon that is evolved during TPO. The fit of the reverse spillover model to the experimental data is shown in Figure S4.

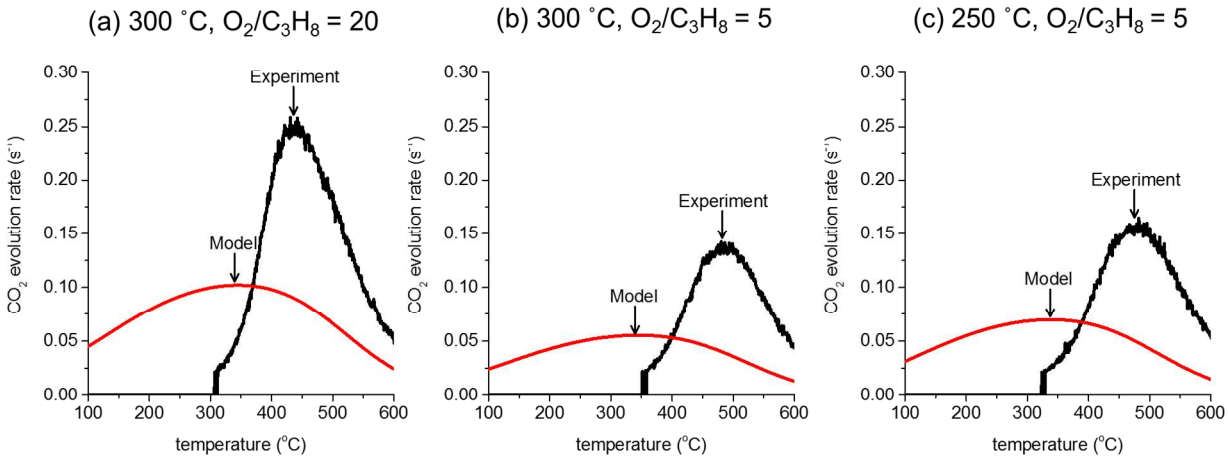

Figure S4. Experimental (black) and simulated (red) CO_2 evolution rates during temperature programmed oxidation of Pt/Al_2O_3 following 8 hours of propane oxidation at (a) 300 ˚C with O_2/C_3H_8 = 20, (b) 300 ˚C with O_2/C_3H_8 = 5, and (c) 250 ˚C with O_2/C_3H_8 = 5. The simulated TPO profiles were calculated using the reverse spillover model, equation S3, with the diffusion rate constants, equation S2, that were extracted from kinetic analysis of oxy-carbon surface species spillover.

S.5. Evidence for Pt surface reaction-limited TPO kinetics

In a previous publication[2] we showed that Pt/Al_2O_3 is slowly deactivated during propane oxidation at lower temperatures and higher O_2/C_3H_8 ratios. For example, Figure S5(a) shows the CO_2 production rates during propane oxidation over Pt/Al_2O_3 under conditions which led to deactivation: 200 ˚C with O_2/C_3H_8 equal to 5 (red) and 20 (blue). With O_2/C_3H_8 equal to 5, the CO_2 production rate decreases by ~50% during the first 2 hours of the reaction. With O_2/C_3H_8 equal to 20, the deactivation is much quicker and more severe; 80% of the catalytic activity is lost in the first 0.5 hours of the reaction. Using DRIFTS of adsorbed CO to track the evolution of the platinum nanoparticle structure over the course of the propane oxidation reaction, we showed that the deactivation is due to the slow growth of platinum-oxide films on the surface of the platinum nanoparticles. Furthermore, we showed that a different platinum-oxide phase is formed with O_2/C_3H_8 equal to 5 (PtO) that has different catalytic properties than the platinum-oxide phase that is formed with O_2/C_3H_8 equal to 20 (Pt_3O_4 or PtO_2).

Although different platinum-oxide phases are formed during propane oxidation with O_2/C_3H_8 equal to 5 and 20, the growth of oxy-carbon species on the catalyst surface is relatively insensitive to platinum-oxide formation. Figure S5(b) shows a comparison of the oxy-carbon species growth curves during propane oxidation over Pt/Al_2O_3 at 200 ˚C with O_2/C_3H_8 equal to 5 and 20. The oxy-carbon growth curves with O_2/C_3H_8 equal to 5 and 20 are nearly identical over the entire 8 hours of the reaction. The DRIFTS spectra collected after 8 hours of the reaction with O_2/C_3H_8 equal to 5 and 20 are shown in Figure S5(c) for comparison. There are many different bands in the spectra displayed in Figure S5(c) that are associated with several different oxy-carbon species on the Al_2O_3 support;[1] however, the spectra collected with O_2/C_3H_8 equal to 5 and 20 are nearly identical, which indicates that both the concentration and the composition of

the oxy-carbon species are similar. These results indicate that the growth of oxy-carbon species on Pt/Al_2O_3 support is relatively insensitive to platinum-oxide formation, which further supports our assumption that the growth rate of oxy-carbon species on Pt/Al_2O_3 is limited by the rate of diffusion on the Al_2O_3 support.

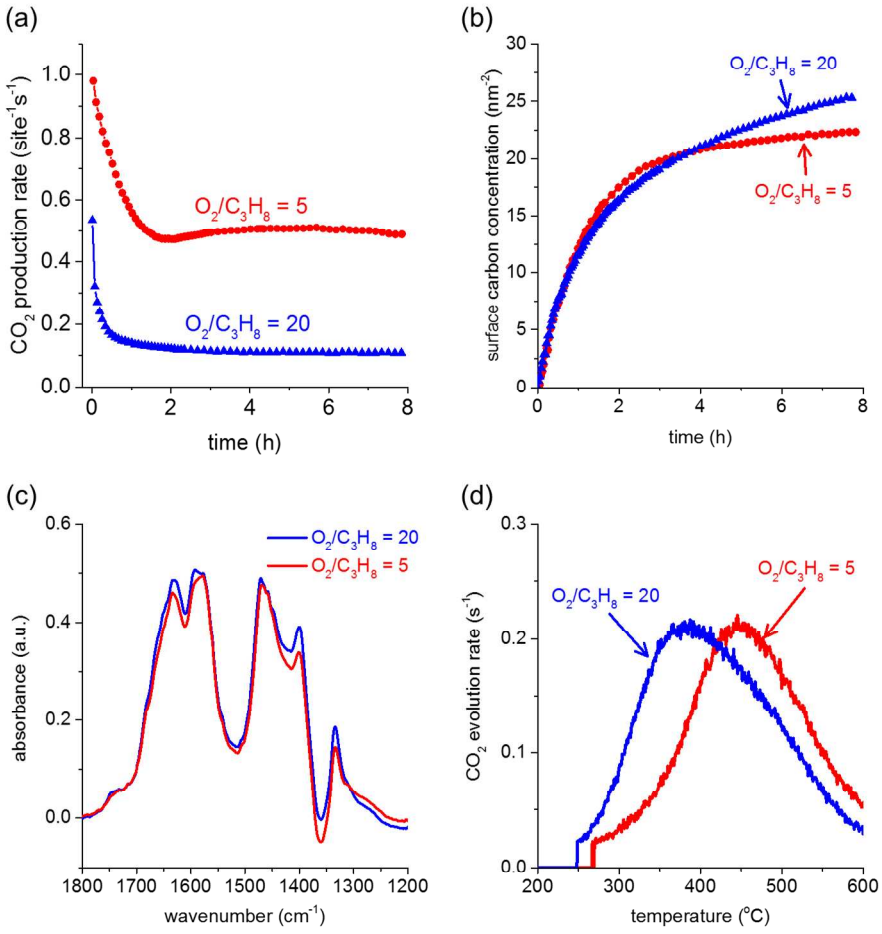

Figure S5. (a) CO_2 production rate (s^{-1}) and (b) surface carbon concentration (nm^{-2}) during propane oxidation over Pt/Al_2O_3 at 200 ˚C with O_2/C_3H_8 equal to 5 (red) and 20 (blue). (c) DRIFTS spectra collected after 8 hours of propane oxidation over Pt/Al_2O_3 at 200 ˚C with O_2/C_3H_8 equal to 5 (red) and 20 (blue). (d) CO_2 evolution rates during temperature programmed oxidation of Pt/Al_2O_3 following 8 hours of propane oxidation at 200 ˚C with O_2/C_3H_8 equal to 5 (red) and 20 (blue). The (a) CO_2 production rates,[2] (b) carbon growth curves,[1] and (c) DRIFTS spectra[1] have been published previously.

Following 8 hours of propane oxidation, the oxy-carbon surface species shown in Figure S5(c) were completely oxidized to CO_2 during temperature-programmed oxidation (TPO), and

the amount of CO_2 evolved during TPO was measured by mass spectrometric analysis of the gas exiting the reactor. The corresponding TPO profiles are displayed in Figure S5(d). If TPO of the oxy-carbon species is a diffusion-limited reaction, then one would expect that the TPO profiles collected following propane oxidation with O_2/C_3H_8 equal to 5 and 20 would be nearly identical because both the concentration and composition of the oxy-carbon species is nearly identical in both cases. However, the oxy-carbon species formed with O_2/C_3H_8 equal to 20 are oxidized at significantly lower temperature than the oxy-carbon species formed with O_2/C_3H_8 equal to 5. This result shows that, in contrast to the growth of oxy-carbon species during propane oxidation, TPO of the oxy-carbon species is influenced strongly by platinum-oxide formation and the platinum-oxide formed with O_2/C_3H_8 equal to 20 (Pt_3O_4 or PtO_2) is more reactive for oxidation of oxy-carbon species than the PtO phase formed with O_2/C_3H_8 equal to 5. Therefore, we can assume that diffusion of the oxy-carbon species is relatively fast during TPO, and the rate limiting step is a chemical reaction taking place on the Pt surface.

Further experimental evidence that TPO of the oxy-carbon species is not a diffusion-limited process is that the initial rate of oxy-carbon species growth on Pt/Al_2O_3 during propane oxidation at 200 ˚C (~0.01 s^{-1}; see Figure S9 in the Supporting Information of our previous work[1]) is more than two orders-of-magnitude higher than their rate of oxidation at 200 ˚C (less than ~$1 \cdot 10^{-4}$ s^{-1}).[1] In other words, the rate of oxidation of the oxy-carbon species is much slower than the rate of oxy-carbon species diffusion on the Al_2O_3 support.

S.6. Temperature-programmed oxidation simulation details

Details of the temperature-programmed oxidation (TPO) simulation procedure have been given in the Supporting Information of a previous publication [1]. The simulation procedure is also described here for convenience. Three different kinetic rate expressions were used to simulate the TPO profiles, each with different reaction orders (1st-order, 2nd-order, and Power-law) with respect to the surface carbon concentration:

1st-order:
$$r_{CO_2,EEA}(T) = \nu_{EEA} \cdot exp\left(\frac{-E_{EEA}}{RT}\right)[C_{EEA}] \quad \text{(S4)}$$

$$r_{CO_2,Ac}(T) = \nu_{Ac} \cdot exp\left(\frac{-E_{Ac}}{RT}\right)[C_{Ac}] \quad \text{(S5)}$$

2nd-order:
$$r_{CO_2,EEA}(T) = \nu_{EEA} \cdot exp\left(\frac{-E_{EEA}}{RT}\right)[C_{EEA}]^2 \quad \text{(S6)}$$

$$r_{CO_2,Ac}(T) = \nu_{Ac} \cdot exp\left(\frac{-E_{Ac}}{RT}\right)[C_{Ac}]^2 \quad \text{(S7)}$$

Power-law:
$$r_{CO_2,EEA}(T) = \nu_{EEA} \cdot exp\left(\frac{-E_{EEA}}{RT}\right)\left[C_{EEA,0}\right] \cdot \left(1 - \frac{C_{EEA}}{C_{EEA,0}}\right)^{n,EEA} \quad \text{(S8)}$$

$$r_{CO_2,Ac}(T) = \nu_{Ac} \cdot exp\left(\frac{-E_{Ac}}{RT}\right)\left[C_{Ac,0}\right] \cdot \left(1 - \frac{C_{Ac}}{C_{Ac,0}}\right)^{n,Ac} \quad \text{(S9)}$$

where $r_{CO_2,EEA}$ represents the rate of CO_2 evolution (s^{-1}) from combustion of EEA species, $r_{CO_2,Ac}$ represents the rate of CO_2 evolution (s^{-1}) from combustion of acetate species, ν_{EEA} represents the pre-exponential factor (s^{-1}) for combustion of EEA species, ν_{Ac} represents the pre-exponential factor (s^{-1}) for combustion of acetate species, E_{EEA} represents the activation energy (kJ/mol) for combustion of EEA species, E_{Ac} represents the activation energy (kJ/mol) for combustion of acetate species, R represents the gas constant (8.314 J/mol/K), T represents the temperature (K), C_{EEA} represents the concentration of EEA species (per-platinum-surface-atom),

C_{Ac} represents the concentration of acetate species (carbon-atoms-per-platinum-surface-atom), $C_{EEA,0}$ represents the initial concentration of EEA species (carbon-atoms-per-platinum-surface-atom), $C_{Ac,0}$ represents the initial concentration of acetate species (carbon-atoms-per-platinum-surface-atom), n, EEA represents the reaction order in the power-law rate expression for EEA species, and n, Ac represents the reaction order in the power-law rate expression for acetate species.

The concentrations of acetate species and EEA species were calculated at each temperature (T_i) that an experimental data point was collected during TPO according to the following equations:

$$c_{EEA}(T_i) = c_{EEA}(T_{i-1}) - r_{CO_2,EEA}(T_{i-1}) \cdot \Delta t \quad \text{(S10)}$$

$$c_{Ac}(T_i) = c_{Ac}(T_{i-1}) - r_{CO_2,Ac}(T_{i-1}) \cdot \Delta t \quad \text{(S11)}$$

where Δt represents the time interval between data points collected (2 seconds).

The initial concentrations of EEA ($C_{EEA,0}$) and acetate ($C_{Ac,0}$) species were calculated from the following equations:

$$C_{EEA,0} = \frac{f_{EEA,0} \cdot C_{total,0} \cdot M_{Pt}}{w_{cat} \cdot D \cdot L} \quad \text{(S12)}$$

$$C_{Ac,0} = \frac{(1 - f_{EEA,0}) \cdot C_{total,0} \cdot M_{Pt}}{w_{cat} \cdot D \cdot L} \quad \text{(S13)}$$

where $C_{total,0}$ represents the total amount (mol) of carbon initially on the surface, which is equal to the total amount of CO_2 evolved during TPO, $f_{EEA,0}$ represents the fraction of the total initial amount of carbon that is EEA species, M_{Pt} represents the atomic mass of Pt (195.09 g), w_{cat}

represents the weight of the catalyst (~0.025 g), D represents the dispersion of the platinum nanoparticles (0.06), and L represents the loading (0.02).

The simulated TPO profiles were then calculated by summing the rates of CO_2 production from combustion of EEA and acetate species at each temperature:

$$r_{CO_2,sum}(T_i) = r_{CO_2,EEA}(T_i) + r_{CO_2,Acetate}(T_i) \quad \text{(S14)}$$

The sum of the squared error between the simulated CO_2 evolution rates ($r_{CO_2,sum}(T_i)$) and the experimental CO_2 evolution rates ($r_{CO_2,exp}(T_i)$),

$$\sum_i \left(r_{CO_2,sum}(T_i) - r_{CO_2,exp}(T_i)\right)^2, \quad \text{(S15)}$$

over all TPO profiles was then minimized by optimizing the adjustable parameters associated with each model (1st-order, 2nd-order, and power-law) using a numerical solver.

For the 1st-order and 2nd-order models, there are 7 adjustable parameters: $log(\nu_{EEA})$, E_{EEA}, $log(\nu_{Ac})$, E_{Ac}, $f_{EEA,0,300-20}$, $f_{EEA,0,300-5}$, and $f_{EEA,0,250-20}$, where $f_{EEA,0,300-20}$ represents the fraction of the total amount of initial surface carbon that is EEA species following 8 hours of propane oxidation at 300 ˚C with O_2/C_3H_8 equal to 20, $f_{EEA,0,300-5}$ represents the fraction of the total amount of initial surface carbon that is EEA species following 8 hours of propane oxidation at 300 ˚C with O_2/C_3H_8 equal to 5, and $f_{EEA,0,250-5}$ represents the fraction of the total amount of initial surface carbon that is EEA species following 8 hours of propane oxidation at 250 ˚C with O_2/C_3H_8 equal to 5. In addition to the 7 adjustable parameters used in the 1st- and 2nd-order models, the power-law model has two more adjustable parameters (n, EEA and n, Ac).

S.7. Parity plots for TPO profiles

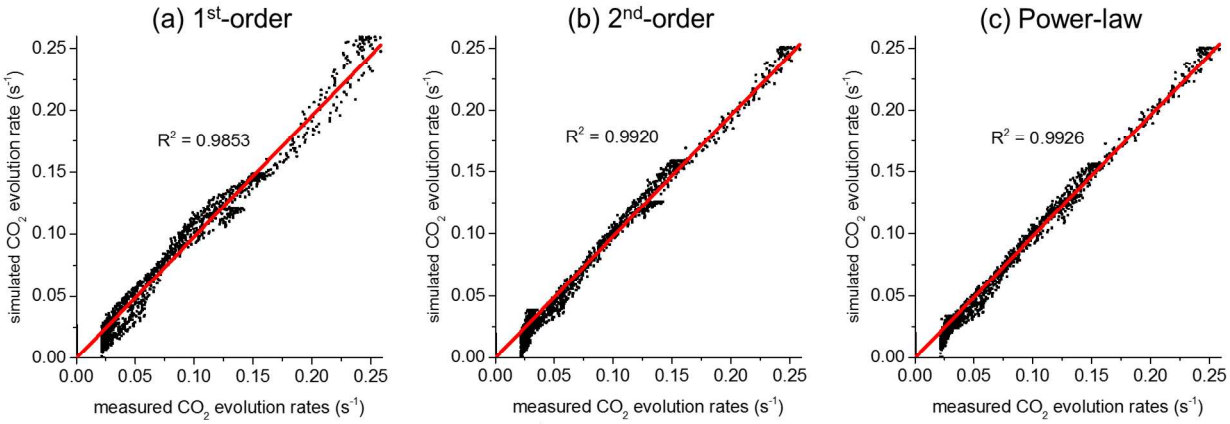

Figure S6. Parity plots for the (a) 1st-order, (b) 2nd-order, and (c) Power-law kinetic models. The experimental and simulated CO_2 evolution rates for each of the models are shown in Figure 3.

S.8. TPO of oxy-carbon species from deactivated Pt/Al_2O_3

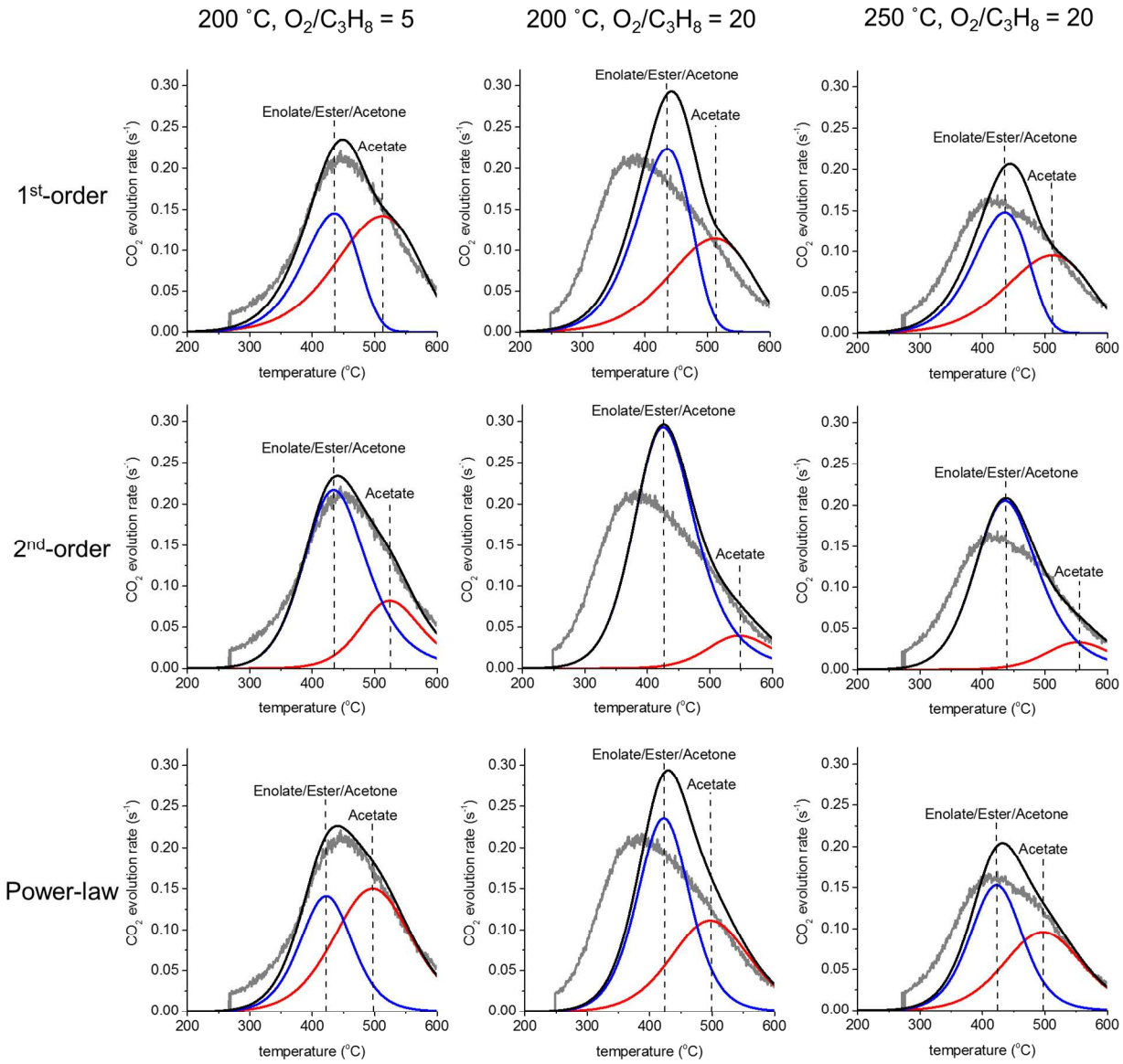

Figure S7. CO_2 evolution rates during temperature programmed oxidation of Pt/Al_2O_3 following 8 hours of propane oxidation under conditions which led to significant catalyst deactivation: (a) 200 ˚C, $O_2/C_3H_8 = 5$, (b) 200 ˚C, $O_2/C_3H_8 = 20$, (c) 250 ˚C, $O_2/C_3H_8 = 20$. The experimental CO_2 evolution rates (grey lines) were simulated using the 2nd-order kinetic model with kinetic parameters listed in Table 1. The simulated TPO profiles (black lines) were calculated from the sum of the TPO profiles for acetate (red lines) and enolate, ester and acetone species (blue lines).

S.9. Parity plot for TPO of oxy-carbon species on the deactivated Pt/Al_2O_3 catalyst

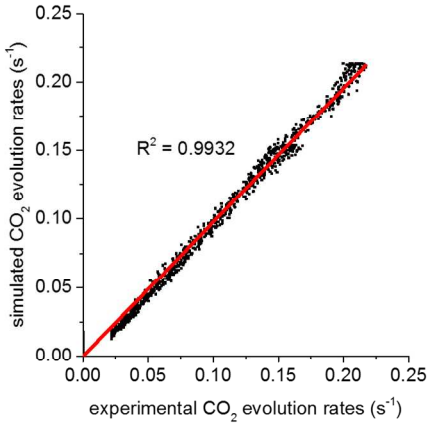

Figure S8. Parity plot of the simulated and experimental CO_2 evolution rates during TPO of oxy-carbon species from Pt/Al_2O_3 catalyst following propane oxidation under conditions which led to catalyst deactivation (O_2/C_3H_8 equal to 20 at 200 ˚C and 250 ˚C). The experimental and simulated CO_2 evolution rates for each of the models are shown in Figure 4.

References

(1) O'Brien, C. P.; Lee, I. C. A Detailed Spectroscopic Analysis of the Growth of Oxy-Carbon Species on the Surface of Pt/Al_2O_3 During Propane Oxidation. *J. Catal.* **2017**, *347*, 1-8.

(2) O'Brien, C. P.; Jenness, G. R.; Dong, H.; Vlachos, D. G.; Lee, I. C. Deactivation of Pt/Al_2O_3 During Propane Oxidation at Low Temperatures: Kinetic Regimes and Platinum Oxide Formation. *J. Catal.* **2016**, *337*, 122-132.